

Matthew D. Eastin\*  
 Colorado State University, Fort Collins, Colorado

1. INTRODUCTION

The amount of buoyancy in a tropical cyclone eyewall and its importance to the lifecycle of the system has been widely debated in recent years. Ooyama (1982) argues that positive buoyancy must exist within the secondary circulation of a tropical cyclone (hereafter referred to as TC) in order to produce the observed strong entrainment, or convergence, into the eyewall above the boundary layer. Ooyama further argues that entrainment into the eyewall above the boundary layer, or positive buoyancy, is necessary for the TC to intensify. Gray (1997) argues that buoyancy in the eyewall must be substantial and must increase with TC intensity so as to balance mass and momentum requirements. Zipser and Lemone (1980) showed that near the eyewall of a mature hurricane 800 J/kg of available energy existed for buoyant upward displacements, hence positive Convective Available Potential Energy (CAPE). With a water loading correction, CAPE can be expressed as:

$$CAPE \equiv \int_{LCL}^{EL} \frac{g}{T_{ve}}(B)dz \quad (1)$$

$$B = T_{vp} - T_{ve}(1 + r_l) \quad (2)$$

where  $LCL$  is the lifted condensation level,  $EL$  is the equilibrium level,  $B$  is the buoyancy force on a parcel at a given level,  $r_l$  is the total liquid water content,  $T_v$  is the virtual temperature, and  $p$  and  $e$  refer to the parcel and environment respectively. Black et al. (1994) argued that buoyant updrafts must exist in the eyewall to explain observed vertical motions on the order of 10 m/s, however, computations of CAPE are likely inaccurate due to water loading, instrument wetting, and difficulty in defining the environment for parcels maintained in a large radial temperature gradient.

Jorgensen and LeMone (1989) utilized a  $CO_2$  radiometer onboard the NOAA WP-3D research aircraft to indirectly sense in-cloud temperatures and calculate parcel buoyancy without the evaporative cooling effects typically experienced by immersion thermometers. In the present study, a  $CO_2$  radiometer is also used to produce thermodynamic radial profiles through numerous TCs to examine the extent of instrument wetting and the potential for error

\*Corresponding Author Address: Matthew D. Eastin, Department of Atmospheric Science, Colorado State University, Fort Collins, CO 80523; e-mail: eastin@mpi.atmos.colostate.edu

Hurricane	Flts	Radial Legs					Total
		900	850	700	600	500	
Diana 84	5		45				45
Danny 85	2		12				12
Elena 85	6		68				68
Gloria 85	7		10	30		6	48
Juan 85	2		17				17
Emily 87	2			13	1	36	50
Floyd 87	1		12				12
Florence 88	2	18					18
Gilbert 88	5		16	28			44
Joan 88	1		6				6
Dean 89	1	4			8		12
Gabrielle 89	1	4		8			12
Hugo 89	4				22	4	26
Jerry 89	1	7					7
Gustav 90	4		6	30			36
Bob 91	1					4	4
Claudette 91	2			20			20
Emily 93	3					15	15
Erin 95	1			16			16
Iris 95	2				4		7
Opal 95	1				4		4
Edouard 96	2			22			22
Norbert 84	6		6	34		25	65
Jimena 91	3		2	17	4		23
Tina 92	4		19				19
Olivia 94	2				15		15
Atlantic	64	33	192	167	42	65	501
E. Pac.	15		27	51	19	25	122
Total	79	33	219	218	61	90	623

Table 1: Summary of Atlantic and East Pacific hurricane radial legs with corrected temperatures by storm, with the number of flights (Flts.), and pressure level. Two radial legs at 400 mb for Gloria 85 were not in the table but were included in the totals.

in estimating the amount of parcel buoyancy in the TC eyewall.

2. AIRBORNE THERMOMETERS

To apply classic parcel theory, accurate thermodynamic measurements must be made both in and out of an updraft to determine if the updraft is buoyant. Direct observations of air temperature within clouds have been attempted by placing an immersion thermometer (typically a platinum wire within a housing) into the airstream. Immersion thermometers are affected by compressional and viscous heating as air approaches the sensing element, there by the sensor does not measure the desired static air temperature ( $T_o$ ) but rather the slightly warmer dry recovery temperature ( $T_r$ ) (neglecting local heating effects). The extent of this warming is a function of the adiabatic deceleration of air from the free-stream airspeed ( $U_o$ ) to some fraction ( $a$ ) of that airspeed. Hence, the static air temperature is obtainable by:

$$T_o = T_r - r \frac{U_o^2}{2c_p} \quad (3)$$

where  $c_p$  is the specific heat of air at constant pressure and  $r=1-a_2$  is the effective recovery factor (typically  $r = 1.0$ ). This correction is applied throughout the flight, yielding reliable temperatures in clear air.

If the sensor unknowingly becomes wet from impinging cloud or precipitation particles, the sensor will acquire the wet-bulb temperature of its environment. The environment is always subsaturated due to compressional heating of the air, thus evaporation of liquid or ice on the sensor ensues. The evaporation results in an erroneously cool temperatures. Lawson and Cooper (1990) combined the effects of dry convective heat transfer for high speed flow around a cylindrical element and wet-bulb psychrometry. They argue that the error caused when the sensor becomes wet is the difference between the equilibrium wet-bulb temperature of the sensor and the recovery temperature, and can thus be calculated. Accounting for air density changes due to adiabatic compression, the temperature error due to completely wet sensor is given by:

$$T_{wb} - T_r = \frac{1}{AP_r} \left( \frac{P_r}{P_o} e_o - e_s(T_{wb}) \right) \quad (4)$$

In (3),  $T_{wb}-T_r$  is the error caused by sensor wetting,  $P_r$  is the total pressure at the sensor surface,  $P_o$  and  $e_o$  are the total pressure and water vapor pressure in the free airstream respectively,  $e_s$  is saturation vapor pressure at the sensor temperature,  $T_{wb}$  is the temperature of the wetted sensor, and

$$A = \frac{C_p}{\epsilon L} \left( \frac{S_c}{P_r} \right)^{0.56} \left( 1 - \frac{\epsilon e_s(T_{wb})}{P_o} \right) \quad (5)$$

is the psychometric parameter for a cylindrical sensor,  $\epsilon$  is the ratio of molecular weights of water to air,  $L$  is the latent heat of vaporization,  $S_c$  is the Schmidt number, and  $P_r$  is the Prandtl number. By combining (3)-(5), the magnitude of the error for a completely wetted sensor becomes a function of aircraft speed, temperature, pressure, and ambient relative humidity. This analytic correction can not usually be applied because of uncertainties in the amount of wetting, but can provide a theoretical upper-limit. Errors during TC penetrations can be as large as 5-7 K for typical aircraft speeds (120-140 m/s), flight levels, temperatures, and humidity conditions. If sub-freezing temperatures and supercooled droplets are encountered, the additional effects of sublimation can result in errors on the order of 10K.

Infrared radiometers can indirectly measure flight-level air temperature along a narrow, short horizontal path utilizing a bandpass filter centered on either the 4.255  $\mu\text{m}$  or 15  $\mu\text{m}$   $CO_2$  absorption band. Albrecht et al. (1979), using the 15  $\mu\text{m}$  band, found that 90% of the signal reaching the instrument was from a path within 200 m from the plane. However in a stratus cloud with liquid water content of 0.2  $\text{g}/\text{m}^3$ , 90% of the signal originated within 33 m from the plane. Thus, assuming a dry (moist)

adiabatic lapse rate in clear (cloudy) air, aircraft roll must (need not) be considered. Liquid water also emits continuum radiation in the  $CO_2$  absorption bands, rendering the measured temperature a weighted average between the drops and air. Supersaturations in updrafts are very small; thus temperatures of growing drops are within 0.1 K of the air temperature. Evaporating drops may be cooler than their environment by as much as 1 K, depending upon liquid water content and relative humidity. Thus, on cloud edges and in subsaturated regions containing precipitation, the weighted average temperature may be too-cool. Radiometers are not susceptible to wetting errors, do not disturb the air, provide a faster response time, and thus are ideal for in-cloud temperature measurements.

### 3. DATA AND ANALYSIS METHOD

The data used in this study were obtained from Hurricane Research Division (HRD) archives. The data were collected by WP-3D aircraft during 79 flights through 26 TCs over 13 years (1984-1996) in the Atlantic and East Pacific basins. Flight-level air temperatures derived from a  $CO_2$  side-looking radiometer (SR) and a Rosemount immersion thermometer (IMT) were obtained with a temporal resolution of 5s along with dewpoint temperatures ( $T_d$ ) measured by a cooled-mirror hygrometer, and aircraft roll data. A 10s running Bartlett filter was applied to the original 1s data to remove high frequency oscillations. Previously processed flight-level radial legs with 0.5 km resolution (Willoughby et al. 1984) were used to represent the three dimensional wind field.

The majority of the data were not accompanied by rain and cloud particle measurements sufficient to directly deduce if instrument wetting were occurring. Hence, instrument wetting was deduced from the 5s IMT and  $T_d$  temperatures since the IMT will be erroneously cool and the  $T_d$  may be erroneously high (see Jorgensen and Lemone, 1989). If the  $T_d$  was within 0.3 K or exceeded the IMT, the data were suspected of instrument wetting errors, otherwise the data were considered in clear air. The SR instrument is known to drift with time. This is removed by applying linear regression to the IMT and SR clear air data during each eye penetration. Data with the aircraft roll exceeding  $3^\circ$  from the horizontal were not used; leaving, on average, 200 data points for each regression. If a high correlation ( $>0.9$ ) of the SR and IMT clear air existed, the regression equation was then applied to all the SR data in the penetration to remove the drift. A relative humidity of 99% was assumed for data suspected of wetting errors and the  $T_d$  was adjusted accordingly for each the SR and IMT. The data were then adjusted along a moist adiabat to a reference pressure level in accordance with the previously processed radial legs. The adjusted 5 s data were "fit" to the 0.5 km resolution radial legs, thus providing a data set with three-dimensional winds and thermodynamics

corrected for instrument wetting. A summary of the radial legs with corrected temperatures used in this study is shown in Table 1. An example of a radial leg with IMT and SR corrected temperatures is shown in Figure 1.

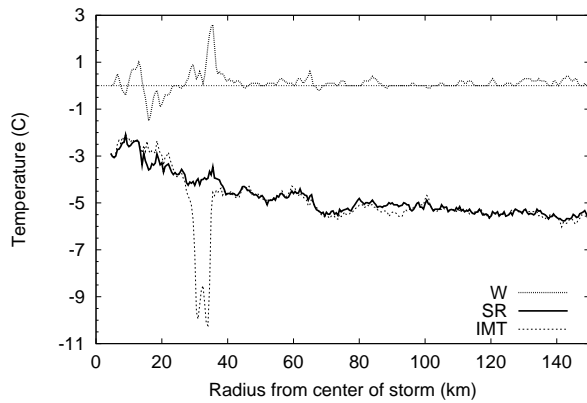


Figure 1: Radial leg for Hurricane Gloria on September 22, 1985 at 500mb with IMT and SR temperatures ( $^{\circ}\text{C}$ ) along with vertical motion (W)(m/s)

## 4. RESULTS AND DISCUSSION

### 4.1 Observed Instrument Wetting

Regions of significant instrument wetting were deduced from the corrected IMT and SR radial leg data. An instrument wetting location (IWL) was defined as a region where the IMT was cooler than the SR by 3 times the clear-air standard deviation of the IMT-SR difference for 5 consecutive data points (2.5 km). Even with this strict definition, 50% of the legs in Table 1 contained an IWL. Shown in Figure 2 is the maximum temperature error for all IWLs. Observed errors rarely reach their theoretical value, suggesting the sensor never becomes completely wetted. The effects of supercooled water can be seen as errors significantly increase near the freezing level.

To determine the effects of instrument wetting within the eyewall updraft, the data was composited in relation to the Radius of Maximum Updraft (RMU) found within 20km on either side of the Radius of Maximum azimuthal Wind (RMW). Over 80% of the IWLs identified (Fig. 2) are within 20 km of the RMU, or 39% of all radial legs contain a IWL within 20 km of the RMU. Average temperature errors at the RMU (Figure 3) indicate that the average eyewall parcel is more than 0.4 K warmer than would be measured by the immersion thermometers. With the results statistically significant with 99.9% confidence at each level, virtual temperatures in updrafts would be warmer by the same magnitude and equivalent potential temperatures warmer by 2-8 K. It should be note that a similar RMU composite for all

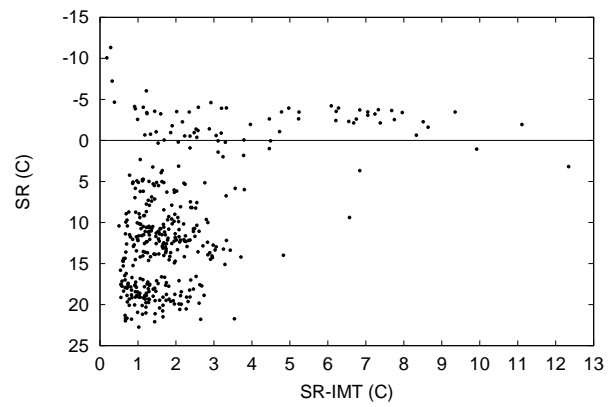


Figure 2: Maximum errors (SR-IMT) ( $^{\circ}\text{C}$ ) found in each identified IWL as a function of temperature.

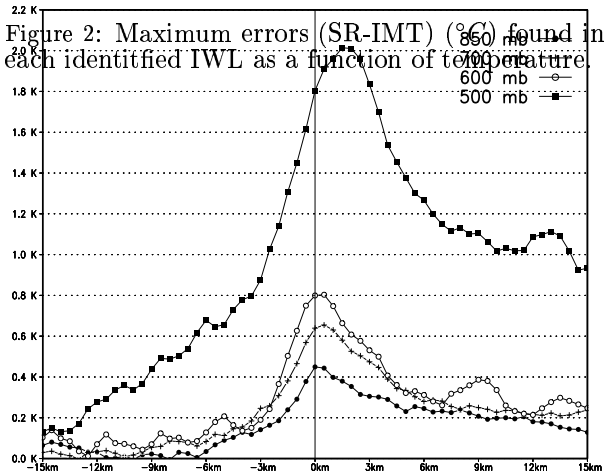


Figure 3: Average temperature error (SR-IMT)( $^{\circ}\text{C}$ ) composited with respect to relative distance from the RMU for all radial legs at the 850-500 mb levels.

radial legs without an IWL still indicated a 0.1-0.2 K wetting error at the RMU with confidence error at the RMU for all radial legs at the 850-500 mb levels greater than 90% for each of the 850-500 mb levels.

### 4.2 Buoyancy

Traditionally, a parcel environment has been defined either, from a sounding in clear air near the convection or the clear air adjacent to the cloud. This practice may be easily applied to general tropical convection where the surrounding environment is uniform. However, the presence of the warm core in a developed hurricane presents a thermally non-uniform environment for eyewall parcel ascent. The parcel is warmer than the outer environment, but cooler than the warm-core eye. Average radial profiles of SR temperature (not shown) indicates that the RMU temperature is equivalent to 50% of the temperature rise between the environment and the eye, with the strongest radial temperature gradient just outside the RMU. Thus, the local eyewall up-

draft environment can be derived from the average gradient in which it is located.

In this study, the parcel environment was defined by applying a 20 point (10 km) running mean to the temperature data of each radial leg. With updraft cores ( $w > 1$  m/s for at least 0.5 km) typically less than 5 km in horizontal extent, the definition of the environment seems reasonable. The parcel buoyancy is calculated at the reference pressure level from (2) for all updraft cores at the RMU. The water loading correction was only applied for cloud water (drop diameters  $< 0.04$  millimeters) due to lack of precipitation measurements for the data set. The distribution of parcel buoyancy calculated from the IMT data (Figure 4) shows that 75% of the updrafts are *negatively* buoyant, thus suggesting the eyewall would resist updrafts on average. This result would not support the observed deep convection that is persistent in the eyewall. The distribution of parcel buoyancy calculated from the SR data (Figure 5) shows that 56% of the updraft cores are *positively* buoyant. This result would support the observed deep convection in the eyewall. While the distribution is not statistically significant (confidence is  $\approx 50\%$ ) for positively buoyant updrafts on average, it does suggest that buoyancy exists within the eyewall. Due to the tendency of pilots to avoid the high reflectivity cores (strong updrafts) during airborne eyewall penetrations, the distribution may be in reality skewed more toward positive buoyancy.

## 5. CONCLUSIONS AND FUTURE WORK

Instrument wetting errors on the order of 0.5K or greater typically occur for immersion thermometers during TC eyewall penetration. The use of a  $CO_2$  radiometer for in-cloud temperature measurements has been shown to have a substantial impact on calculated updraft parcel buoyancy values. Roughly half of the eyewall updraft cores sampled were positively buoyant. These results agree with previous studies (e.g. Black et al. 1994) that buoyant convection must occur in the eyewall. Further analysis and stratification of the data is planned to investigate variations of TC buoyancy with intensity, lifecycle, and location in the storm.

*Acknowledgments.* I wish to thank Dr. William Gray, Dr. Peter Black and Dr. Bob Black for many helpful discussions. Funding was provided by NSF under Contract ATM-9616818.

## REFERENCES

- Albrecht, B. A., S. K. Cox and W. H. Schubert, 1979: Radiometric measurements of in-cloud fluctuations. *J. Appl. Meteor.*, **18**, 1066-1071.
- Black, R. A., H. B. Bluestein, and M. L. Black, 1994: Unusually strong vertical motions in a Caribbean hurricane. *Mon. Wea. Rev.*, **122**, 2722-2739.
- Gray, W. M., 1997: The tropical cyclones Maximum Potential Intensity (MPI). Preprints, *22nd Conf. on Hurricanes and Tropical Meteorology*, Fort Collins, CO, Amer. Meteor. Soc., 288-289.

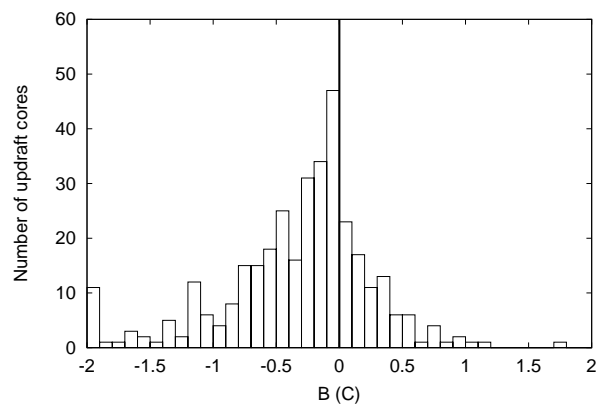


Figure 4: Distribution of flight level parcel buoyancy ( $B$ ) ( $^{\circ}C$ ) calculated from the IMT data at the RMU using Equation 2.

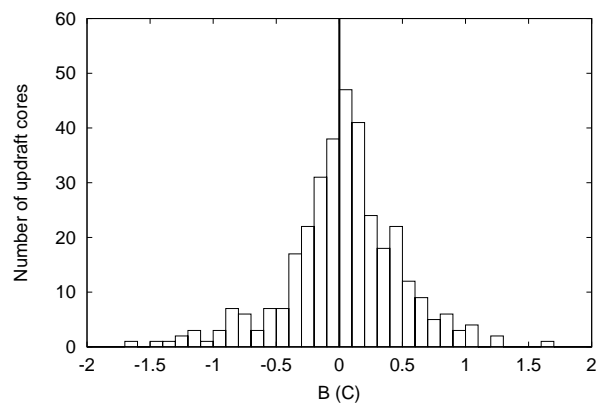


Figure 5: Distribution of flight level parcel buoyancy ( $B$ ) ( $^{\circ}C$ ) calculated from the SR data at the RMU using Equation 2.

- Jorgensen, D. P., and M. A. Lemone, 1989: Vertical velocity characteristics of oceanic convection. *J. Atmos. Sci.*, **46**, 621-640.
- Lawson, R. P., and W. A. Cooper, 1990: Performance of some airborne thermometers in clouds. *J. Atmos. Oceanic Technol.*, **7**, 480-494.
- Ooyama, K. V., 1982: Conceptual evolution of the theory and modeling of the tropical cyclone. *J. Meteor. Soc. Japan*, **60**, 369-380.
- Willoughby, H. E., F. D. Marks, Jr. and R. J. Feinberg, 1984a: Stationary and moving convective bands in hurricanes. *J. Atmos. Sci.*, **41**, 3189-3211.
- Zipser, E. J., and M. A. Lemone, 1980: Cumulonimbus vertical velocity events in GATE. Part II: Synthesis and model core structure. *J. Atmos. Sci.*, **37**, 2458-2469.